Supporting online text

1. To isolate mutant strains defective in the activation of *PHO5* transcription, we treated the parental strain [EY696 (K699 *MAT**a** pho80^{ts} can1::pPHO5-CAN1 pho81Δ::TRP1B ade2-1 trp1-1 leu2-3, 112 his3-11, 15 ura3-1*)] with ethylmethane sulfonate to ~50% viability and plated it for growth on SD - arginine + 8 μg/ml canavanine medium at 37°C. Cells with *pPHO5-CAN1,* a *PHO5* promoter-*CAN1* fusion construct, are sensitive to canavanine in conditions that induce *PHO5* expression. We isolated 20 mutants carrying recessive mutations affecting Pho5 acid phosphatase activity. Ten of these were divided into four complementation groups, with the remaining ten unassigned. Four mutants with mutations in *PSE1* or *ARG82* displayed defects in *PHO5* transcription. The remaining 16 mutants were found to contain defects in Pho5 activity that are downstream of transcription, and were not examined further.

2. The *arg82-153* allele was recovered by gap repair of two different gapped vectors. The rescued allele from each vector was determined to be identical in the *ARG82* coding region by sequencing. *arg82-153* contained a single C to T substitution at position 541, introducing a stop codon following the inositol-binding motif, and failed to rescue the *PHO5* uninducible phenotype of *arg82Δ* cells. Since the *arg82-153* allele rescued the temperature-sensitive lethality of the *arg82Δ* strain (2, 5), it is unlikely to be a null.

3. *PHO5* and *PHO84* expression is partially constitutive in the following strains, grown in high phosphate conditions: *plc1Δ pho80^{ts}*, *arg82Δ pho80^{ts}*, and *kcs1Δ pho80^{ts}* (2). This partially constitutive expression is dependent on *PHO81*, suggesting that inositol polyphosphates may play a role in the phosphate signaling pathway upstream of

the CDK inhibitor Pho81. This additional role for inositol polyphosphates may also be the cause of increased binding of Ino80, Snf2, and Pho4 to the *PHO5* and *PHO84* promoters in the *arg82Δ* strain (Figs. 2c, 2d, 3a, and S4, DMSO WT vs. *arg82Δ*), as these experiments were carried out using a strain that is $PHO81^{+}$.

4. Snf2 and Ino80 are the catalytic subunits of the SWI/SNF and INO80 remodeling complexes, respectively. Because *ino80Δ* and *snf2Δ leu2-3 trp1-1* strains are not viable in K699 yeast, we deleted nonessential components that impair function of the remodeling complexes.

5. We use the $Pho85^{F82G}$ strain to control transcription of phosphate-responsive genes because addition of 1-NaPP1 to cells inhibits Pho85 function within minutes (7) and is a more selective perturbation of the pathway than shifting $pho80^{ts}$ cells to 37°C. Like the *arg82Δ pho81Δ* $pho80^{ts}$ strain, *arg82Δ* $Pho85^{F82G}$ cells are also defective for *PHO5* transcription and chromatin remodeling (2).

6. We find that strains with mutations in *SNF6* and *SNF2* induce *PHO5* transcription with slower kinetics when depleted for phosphate (2). A defect in *PHO5* transcription induction in no phosphate medium has been previously reported for an *ino80Δ* strain (8). In general, mutations in subunits of the SWI/SNF and INO80 complexes impair *PHO5* induction to a lesser degree when cells are depleted of phosphate versus treated with 1-NaPP1 in high phosphate (2). This is consistent with an earlier report (9) proposing that an additional signal(s), independent of Pho80-Pho85, contributes to activation of *PHO5* transcription when cells are starved for phosphate.

7. Gcn5- and Esa1-containing histone acetyltransferase (HAT) complexes acetylate histones H3 and H4 at the *PHO5* promoter and regulate its transcription (10-12). We did

not observe detectable changes in the acetylation levels of histones H3 or H4 at the *PHO5* promoter in *arg82Δ* cells, suggesting that Gcn5 and Esa1 function may not be influenced by inositol polyphosphates (2).

Supporting figures

Figure S1

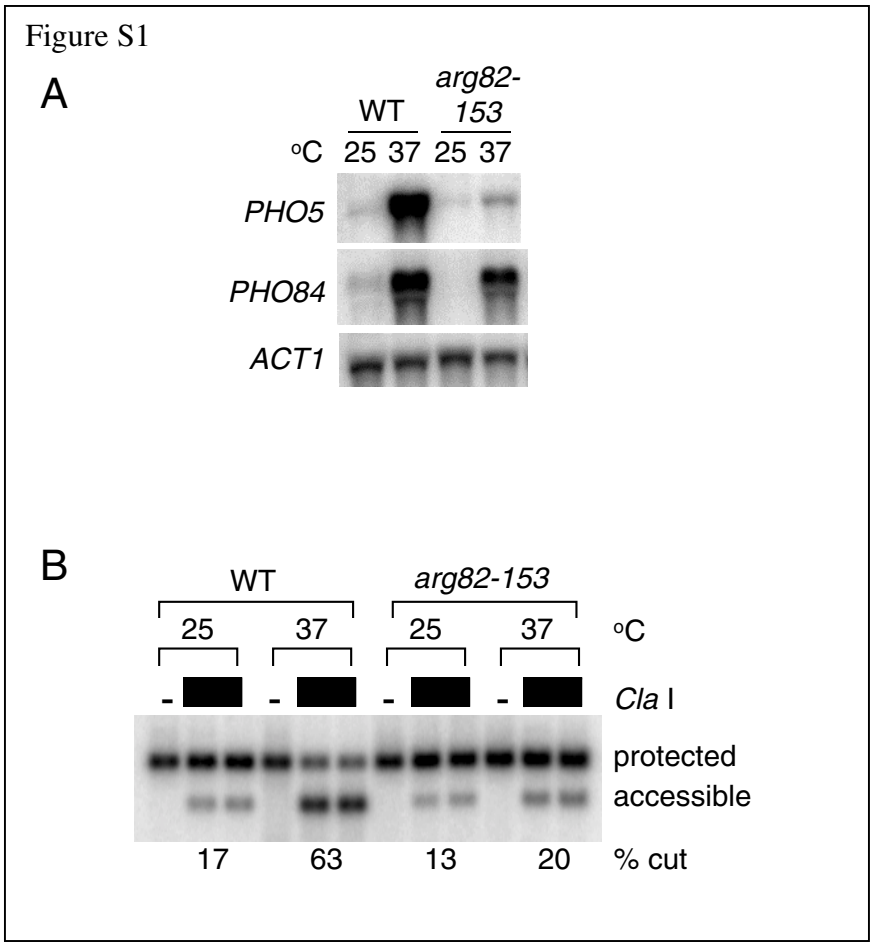

Figure S1. The *arg82-153* mutant is defective in *PHO5* mRNA induction and chromatin remodeling. To control induction of the *PHO5* gene, which encodes a secreted acid phosphatase, a strain carrying a temperature sensitive allele of *PHO80* was used (1). In

the *pho80*^{ts} strain, *PHO5* is repressed at the permissive temperature (25°C) and is induced when shifted to the restrictive temperature (37°C). (A) Northern analysis of *pho81Δ pho80*^{ts} (WT) and *arg82-153 pho81Δ pho80*^{ts} strains grown under repressing conditions (25°C) or shifted to inducing conditions (37°C) for one hour. For all experiments, strains were grown in synthetic high phosphate medium and *PHO5* and *PHO84* RNA levels were quantified by normalizing to *ACT1*. The mRNA level in the mutant was 16-fold lower than that in the wild-type strain under inducing conditions. Not all Pho4-dependent, phosphate-responsive genes are affected by the *arg82-153* allele to the same degree; *PHO84*, encoding an inorganic phosphate transporter, was induced to 80% of wild-type levels, suggesting that Pho4 can activate transcription in the *arg82-153* strain. Consistent with a model in which *ARG82* functions downstream of *PHO4*, the subcellular localization of Pho4 is appropriately regulated in the *arg82-153* mutant (2). (B) To determine if the transcriptional defect in the *arg82-153* strain is the result of a block in chromatin remodeling, we examined *Cla* I restriction enzyme accessibility for *pho81Δ pho80*^{ts} (WT) and *arg82-153 pho81Δ pho80*^{ts} strains grown under repressing conditions (25°C) or shifted to inducing conditions (37°C) for one hour. The assay was performed as described elsewhere (3). For all experiments, nuclei were digested with 40 and 160 units of *Cla* I, and equal cutting of each nuclei preparation by the two different amounts of *Cla* I was observed, indicating complete digestion of the accessible templates. Digestion of nuclei with micrococcal nuclease (MNase) revealed that nucleosomes are appropriately positioned under repressing conditions at the *PHO5* promoter in the *arg82-153* mutant (2).

Figure S2

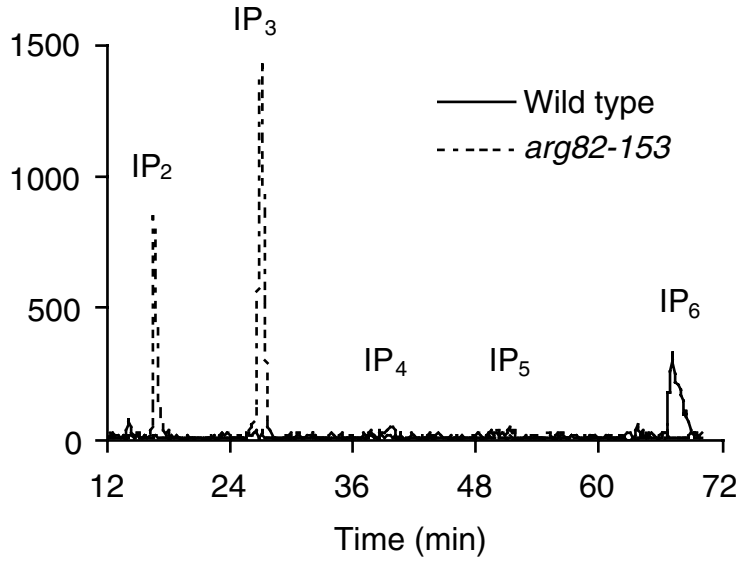

Figure S2. IP_4, IP_5, and IP_6 levels are greatly reduced in the *arg82-153* mutant, suggesting that there is a defect in IP_3 kinase activity in this strain. HPLC analysis of soluble extracts prepared after steady-state [^{3}H]inositol labeling (4) of *pho81Δ pho80^{ts}* (wild-type) and *arg82-153 pho81Δ pho80^{ts}* strains, grown in synthetic high phosphate medium at the permissive temperature (25°C). The elution positions of IP_3, IP_4, IP_5, and IP_6 are indicated. The predominant IP isomer in wild-type yeast from steady-state [^{3}H]inositol labeling is IP_6, whereas cells lacking Arg82 show a loss of IP_4, IP_5, and IP_6, and have increased amounts of IP_2 and IP_3 (5).

Figure S3

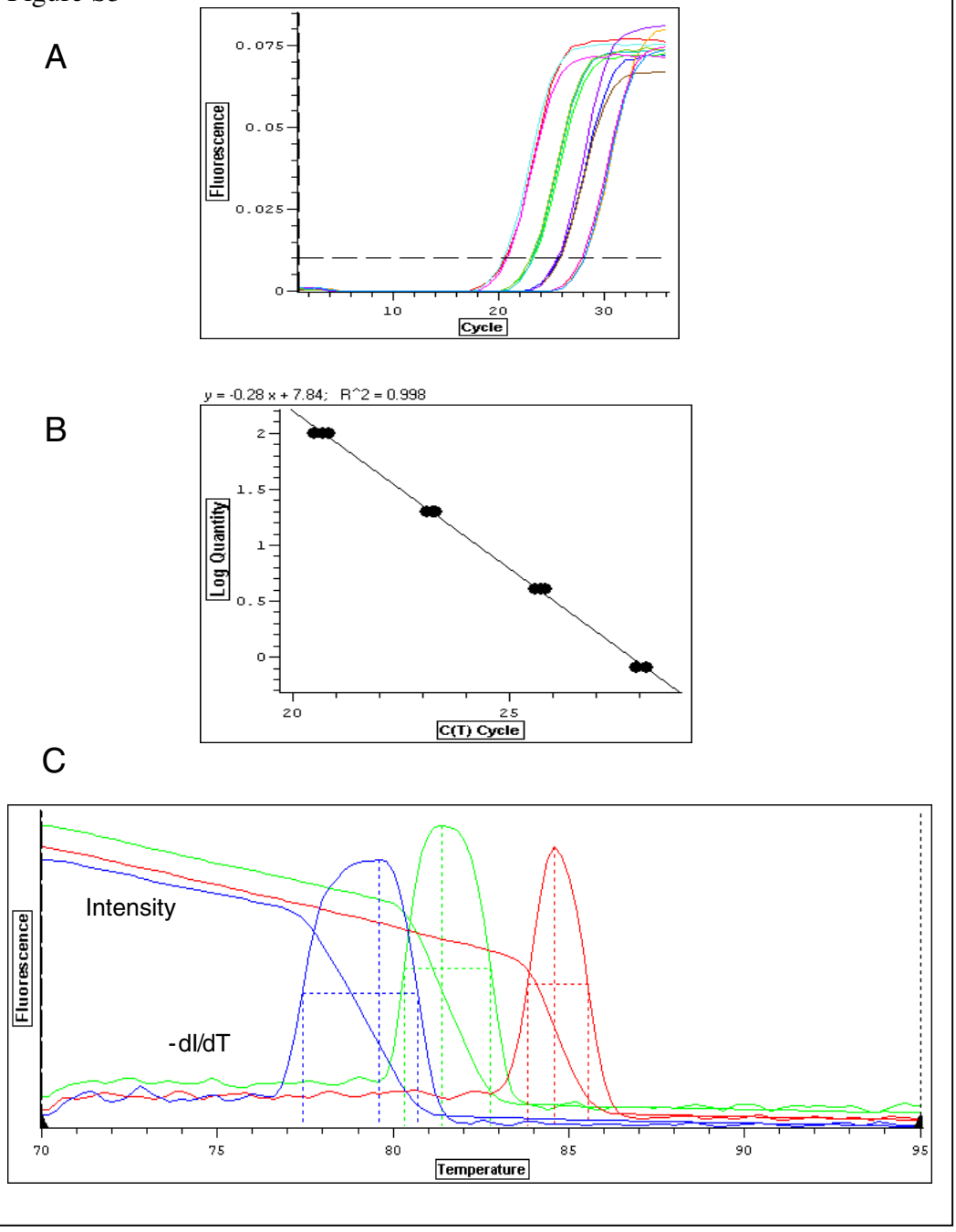

Figure S3. ChIP was performed as described elsewhere (6). Strains were grown under repressing conditions (DMSO) or shifted to inducing conditions by adding 10 µM 1-

NaPP1 for 30 min. Ino80-HA and Snf2-Myc were tagged at the C-terminus with 3 HA and 13 Myc epitopes, respectively, and the gene coding for each was integrated at the native locus. The *PHO5* (-492 to -191 base pairs (bp)), *PHO84* (-460 to -213 bp), and *ACT1* (-142 to +35 bp) promoter DNA sequences were amplified by PCR and quantified by a DNA Engine Opticon System (MJ Research) for continuous fluorescence detection. Each primer pair produced a single DNA fragment of the appropriate size and no detectable primer dimers. (A) Data graph. Input DNA from a randomly-selected ChIP sample was diluted 100-, 500-, 2500-, and 12,500-fold, and an equal volume from each dilution was added to samples containing the *PHO5, PHO84* or *ACT1* primers and subjected to PCR. The fluorescence of SYBR Green I, which is greatly enhanced upon binding dsDNA, is graphed versus cycle number for all 12 reactions. For a given dilution, the *PHO5, PHO84* and *ACT1* primers yield curves that are nearly superimposable, indicating that each amplifies its target with similar efficiency. The position of the cycle threshold (C(T)) is indicated by the dashed line. (B) Standard curve. The initial quantities of template in the serial dilutions were arbitrarily set to 100, 20, 4, and 0.8 to graph the Log Quantity versus the cycle at which the sample's fluorescence crosses the C(T) line. The R-square value of 0.998 indicates that the fit of the linear curve explains 99.8% of the variation in the data. Data from all 12 reactions (*i.e.* from each primer pair) were used to generate the curve. For the experiments in the manuscript, PCR samples of a particular primer pair were quantified using standard curves generated from the same primer pair. (C) Melting curve. Following PCR, the fluorescence intensity (I) was graphed versus temperature (T) for a *PHO5* (green), *PHO84* (red) and *ACT1* (blue) sample. A decrease in fluorescence is observed as the dsDNA melts. Each

of the *PHO5, PHO84* and *ACT1* PCR fragments produces a distinct melting curve corresponding to fragment length and GC content. A single peak generated by graphing –dI/dT versus temperature for each indicates product homogeneity.

Figure S4

A

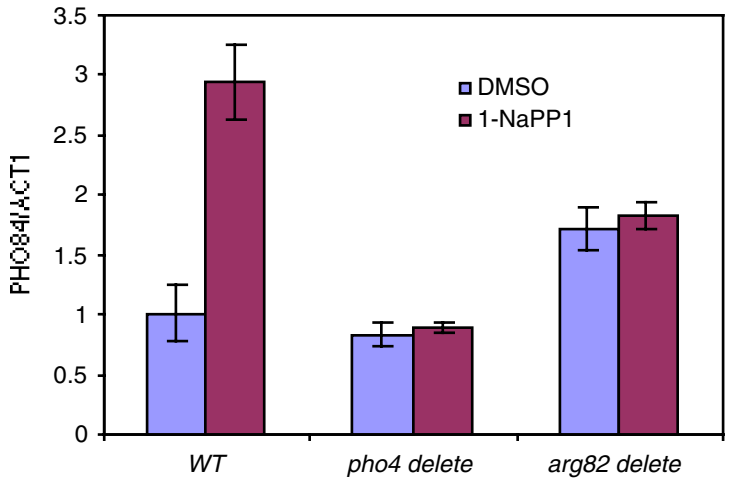

B

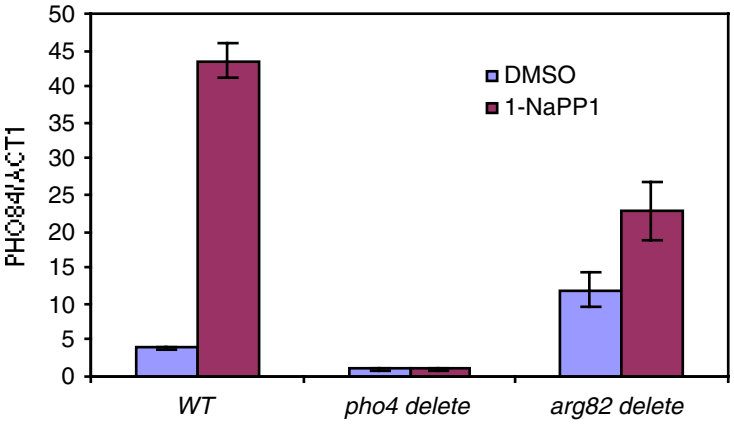

Figure S4. (A) ChIP using a monoclonal antibody that recognizes Ino80-HA in Pho85^{F82G}-expressing strains with the relevant genotypes indicated. (B) ChIP using affinity-purified polyclonal antibodies recognizing Pho4 in Pho85^{F82G}-expressing strains with the relevant genotypes indicated.

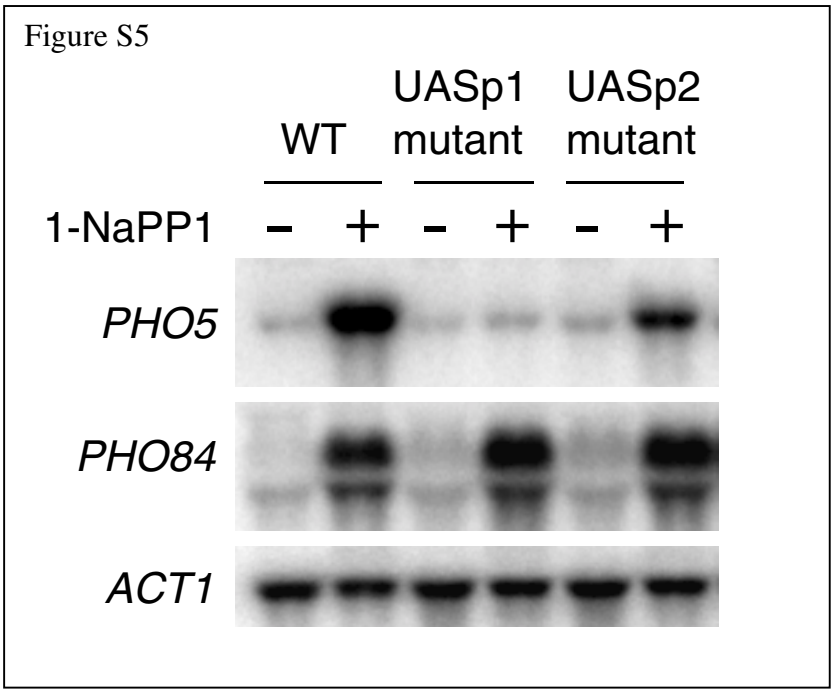

Figure S5. *PHO5* promoter activity is decreased by mutations in UASp1 or UASp2. Northern analysis of Pho85^{F82G}-expressing strains carrying base substitutions in the Pho4-binding sites of UASp1 and UASp2 in the *PHO5* promoter. Mutation of UASp1 resulted in a promoter that is uninducible, while mutation of UASp2 decreased promoter activity 2.5-fold. AAGCTT was substituted for either CACGTT (UASp1) or CACGTG (UASp2), and the mutant alleles were integrated at the native locus. Strains were grown

in repressing conditions (-) or shifted to inducing conditions (+) by adding 10 μM 1-NaPP1 for one hour.

Figure S6

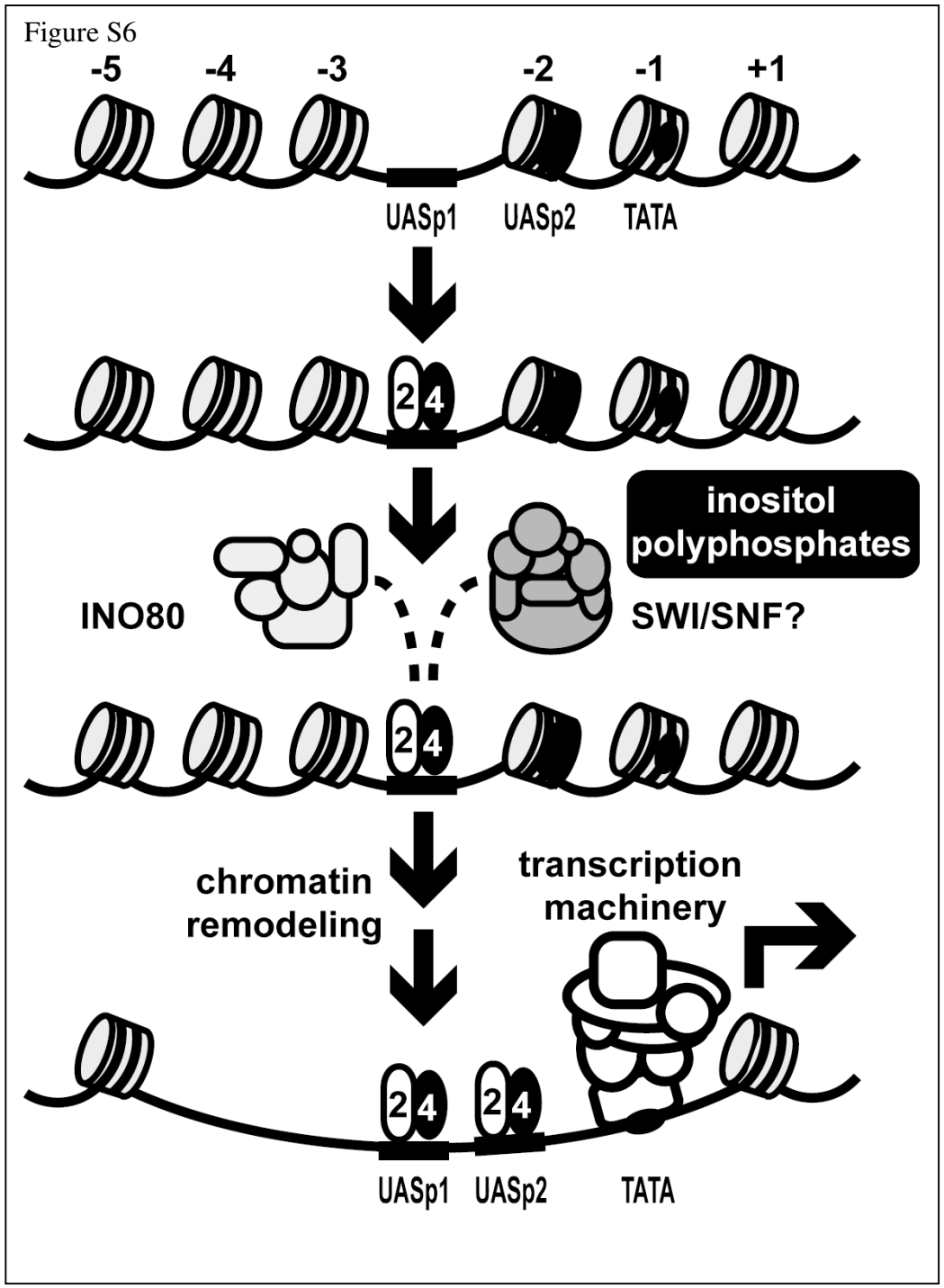

Figure S6. Schematic model illustrating the activation of *PHO5* transcription by ATP-dependent chromatin remodeling complexes. Following import into the nucleus, Pho4 and Pho2 bind to UASp1 in the nucleosome-free region of the unremodeled promoter. In the presence of IP_4/IP_5, Pho4 and/or Pho2 recruit(s) the INO80 complex (and possibly SWI/SNF) to the promoter. This leads to disruption of positioned nucleosomes –1 to –4, greatly increasing the accessibility of UASp2 and the TATA box for binding by Pho4 and $TF_{II}D$, respectively.

References

1. Y. Ueda, E. A. To, Y. Oshima, *J. Bacteriol.* **122**, 911-22. (1975).

2. D. J. Steger, E. S. Haswell, E. K. O'Shea, unpublished data.

3. P. D. Gregory, W. Hörz, *Methods Enzymol.* **304**, 365-76 (1999).

4. J. D. York, A. R. Odom, R. Murphy, E. B. Ives, S. R. Wente, *Science* **285**, 96-100. (1999).

5. A. R. Odom, A. Stahlberg, S. R. Wente, J. D. York, *Science* **287**, 2026-9. (2000).

6. A. Hecht, S. Strahl-Bolsinger, M. Grunstein, *Methods Mol. Biol.* **119**, 469-79 (1999).

7. A. S. Carroll, A. C. Bishop, J. L. DeRisi, K. M. Shokat, E. K. O'Shea, *Proc. Natl. Acad. Sci. USA* **98**, 12578-83. (2001).

8. X. Shen, G. Mizuguchi, A. Hamiche, C. Wu, *Nature* **406**, 541-4. (2000).

9. P. D. Gregory *et al.*, *Mol. Cell* **1**, 495-505 (1998).

10. M. Vogelauer, J. Wu, N. Suka, M. Grunstein, *Nature* **408**, 495-8. (2000).

11. L. Galarneau *et al.*, *Mol. Cell* **5**, 927-37. (2000).

12. S. Barbaric, J. Walker, A. Schmid, J. Q. Svejstrup, W. Hörz, *EMBO J.* **20**, 4944-51. (2001).